PHYSICAL REVIEW B VOLUME 10, NUMBER 8 15 OCTOBER 1974

Neutron diffraction study of KCN III and KCN IV at high pressure*

D. L. Decker,† R. A. Beyerlein, G. Roult,‡ and T. G. Worlton
Argonne National Laboratory, Argonne, Illinois 60439
(Received 27 September 1973)

The high-pressure polymorphs of KCN, KCN III, and KCN IV, have been investigated by neutron diffraction using a polycrystalline sample. High-resolution intensity data have been obtained which confirm the structural description of KCN III but contradict the description of KCN IV suggested by previous high-pressure x-ray work. At a pressure of 25 kbar and at room temperature, KCN IV has a monoclinic structure with the $Cm(C_s^3)$ space group in which the C and N nuclei lie nearly along the body diagonal of a slightly distorted cube of K^+ ions. The conclusion from the x-ray work that KCN IV is rhombohedral is contradicted both by our intensity data and by the fact that several of the diffraction lines are displaced slightly from rhombohedral positions. Increase of the temperature from 66 to 74 °C at a pressure of 22 kbar results in the transformation from phase IV into the cubic phase KCN III with the space group $Pm3m(O_h^1)$ in which the CN^- molecules are ordered randomly along the eight equivalent [111] directions. The temperature factors in KCN III are unusually large indicating a high probability of a CN^- ion jumping between equilibrium positions along the eight diagonal configurations.

I. INTRODUCTION

The pressure-temperature phase diagram of KCN has been reported[1-3] and is shown over a restricted P-T range in Fig. 1. Recent neutron-diffraction measurements[4] confirm that the I-V phase line shown by Pistorius *et al.*[2] is in error as suggested in the note added in proof in that paper and thus it is not shown here. The high-pressure polymorphs KCN III and KCN IV, have been examined by means of x-ray powder techniques[5,6] in an opposed anvil type apparatus, but the limitations of the data left some uncertainty in the structure assignments. Richter and Pistorius[6] report KCN III as cubic, probably space group $Pm3m(O_h^1)$ but their intensity data could not be used to confirm this space-group assignment which was based on analogy arguments from measurements on CsCN and TlCN. They also suggested that the CN^- ions are disordered in KCN III, undergoing either a hindered rotation within the cubes of K^+ ions or a rapid reorientation among the eight equivalent positions along the four body diagonals. This latter structure could lead to a configuration entropy of $R\ln 8$. Neutron-diffraction measurements[4,7] in KCN I strongly suggest that the rotation model is incorrect. Pistorius[5] reported the KCN IV structure to be rhombohedral with the space group $R\bar{3}m(D_{3d}^5)$ and suggested that the linear CN^- ions are oriented but not ordered along the body diagonal. Again the intensities of the x-ray lines could not be used to help determine the space group. The space-group assignment was made using arguments from measurements on CsCN and a possible orientation entropy of $R\ln 2$.[8]

In order to clarify some of the uncertainties in the understanding of these high-pressure phases of KCN, we felt it of interest to measure the diffraction patterns of KCN III and KCN IV (Ref. 9) with the high-pressure neutron-diffraction apparatus[10] now at the CP-5 facility at Argonne. Our measurements confirm the structural description of KCN III but contradict the description of KCN IV suggested by previous high-pressure x-ray work. KCN III is cubic with the space group $Pm3m(O_h^1)$, while KCN IV is monoclinic with the space group $Cm(C_s^3)$ rather than rhombohedral.

Measurements at different pressures and temperatures in phase IV yield a value of $\alpha = (0.22 \pm 0.06)\times 10^{-3}\ ^\circ C^{-1}$ for the volume thermal expansion and $\kappa = (1.43 \pm 0.33)\times 10^{-3}$ kbar^{-1} for the isothermal volume compressibility in this phase. The volume change between KCN III and KCN IV is 0.38 ± 0.07 cm^3/mole at 22 kbar. This may be compared to Bridgman's value[1] of 0.22 cm^3/mole at 23 kbar from a piston-displacement measurement and Richter and Pistorius's value[6] of 0.49 cm^3/mole at 30 kbar from high-pressure x-ray-diffraction work. From our measurement and the slope of the III-IV phase line (0.21 kbar deg^{-1}),[2] the entropy change between these two phases is calculated as $R\ln 2.62$.

The measurement at 22 kbar and 66 °C falls in the region previously reported as KCN III (Ref. 2) and, indeed, we found that the KCN IV → III transition had begun at this temperature and pressure. The most intense KCN III peak, (110), was resolved although barely perceptible in the predominantly KCN IV diffraction pattern.

II. EXPERIMENTAL

A high-purity KCN single crystal which was obtained from Susman and Hinks[11] was crushed with a mortar and pestle, loaded into a die inside a glove box, and pressed into pellets of 0.63-cm

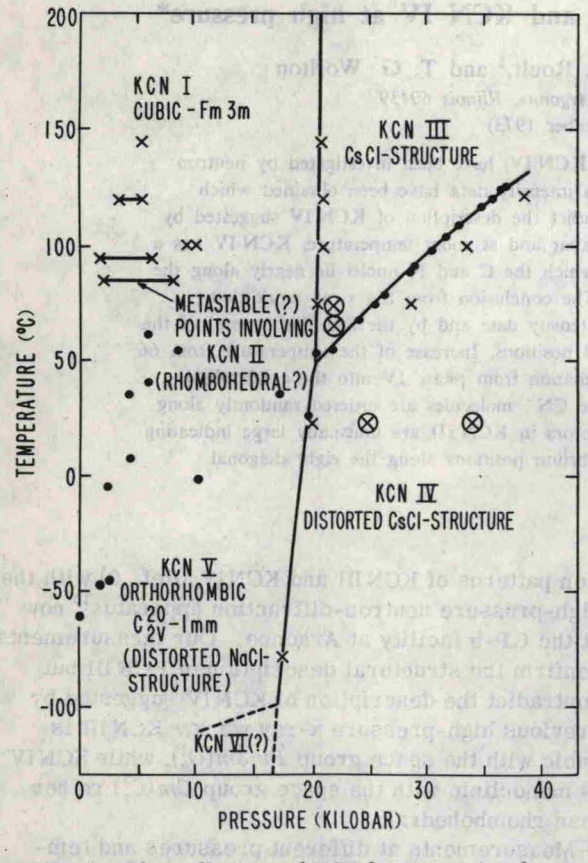

FIG. 1. Phase diagram of KCN for a restricted pressure-temperature range. The ⊗'s mark the P-T points corresponding to the measurements reported here. All other symbols are associated with phase boundary determinations as reported in Ref. 2.

diameter. The pressure apparatus, a double acting piston in cylinder, has been described previously.[9,12] The only new feature was the method of heating the pressure chamber and sample and the temperature control. Water from a large heated bath was pumped through channels in an aluminum jacket around the binding ring. A thermocouple in contact with the outside of the Al_2O_3 pressure chamber was used in a feedback circuit to control an auxiliary heater that kept the thermocouple reading constant to within ±2 °C.

The pressure at the sample was determined from a calibration of the pressure cell. This was accomplished by making several diffraction measurements of either pure NaCl in the sample chamber or mixtures of materials containing NaCl. The pressure was determined from the NaCl lattice spacing using Decker's equation of state.[13] In all cases the pressure versus load was repeatable to within ±0.5 to 30 kbar.

The neutron beam time-of-flight techniques have also been described.[12,14] The time-of-flight spectrometer was calibrated by taking diffraction patterns of Si and Ge (Ref. 15) in the same position as the KCN sample. Diffraction spectra of KCN were taken at the P-T points indicated in Fig. 1. The collection time for the KCN measurements ranged from 28 to 88 h.

The phase changes in our pressure system were clean and sharp with complete disappearance of phase I at 25 kbar and room temperature and complete disappearance of phase IV at 74 °C and 22 kbar. The IV → III transition had barely begun at 66 °C and 22 kbar. These are indications of a good quasihydrostatic environment which is necessary in order to get meaningful intensity data from a powder sample for which one requires there be no preferential orientation of the crystallites.

III. RESULTS AND ANALYSES OF THE DIFFRACTION PATTERNS

Time-of-flight (TOF) neutron-diffraction patterns with scattering angles of 60° are compared in Figs. 2 and 3 for KCN III and KCN IV. The data were initially analyzed by fitting the peaks individually by a least-squares analysis to determine peak position and intensity. Tables I and II show that the positions of the diffraction peaks observed for KCN III are accurately indexed in terms of a simple cubic lattice, while some of the peak positions for KCN IV are displaced slightly from their exact rhombohedral values. This indicates that the actual structure of KCN IV is distorted from rhombohedral symmetry.

To further analyze the TOF data we wrote a computer program that yielded a least-squares fit to the entire spectrum assuming the diffraction peaks are superimposed on a Maxwellian background plus a time-independent background. The count rate, y_i, in the ith time channel is then

$$y_i = b + M(\lambda_i) + \sum_{\vec{h}} \alpha_{\vec{h}} \exp \frac{(-4\ln 2)(d_i - d_{\vec{h}})^2}{S_i^2} + v \sum_{\vec{h}'} f_{\vec{h}'} \exp \frac{(-4\ln 2)(d_i - d_{\vec{h}'})^2}{S_i^2} , \quad (1)$$

where b is the time-independent background; λ_i is the neutron wavelength scattered into channel i; $M(\lambda_i) = \beta d_i^{-\gamma} e^{-\delta/\lambda_i^2}$ is a Maxwellian intensity function with three variable parameters β, γ, and δ used to fit the time-dependent background; d_i is the wavelength scattered into channel i divided by the factor $2\sin\theta$, where 2θ is the scattering angle (30° or 60°); and S_i is the instrumental linewidth at half-peak height for each channel. The symbols $\vec{h}$ and $\vec{h}'$ stand for the Miller indices (hkl) for the KCN peaks and for the Al_2O_3 peaks, respectively, which might be present in the pattern. The calculated plane spacings for KCN and Al_2O_3, $d_{\vec{h}}$ and $d_{\vec{h}'}$, respectively, are determined from the lattice param-

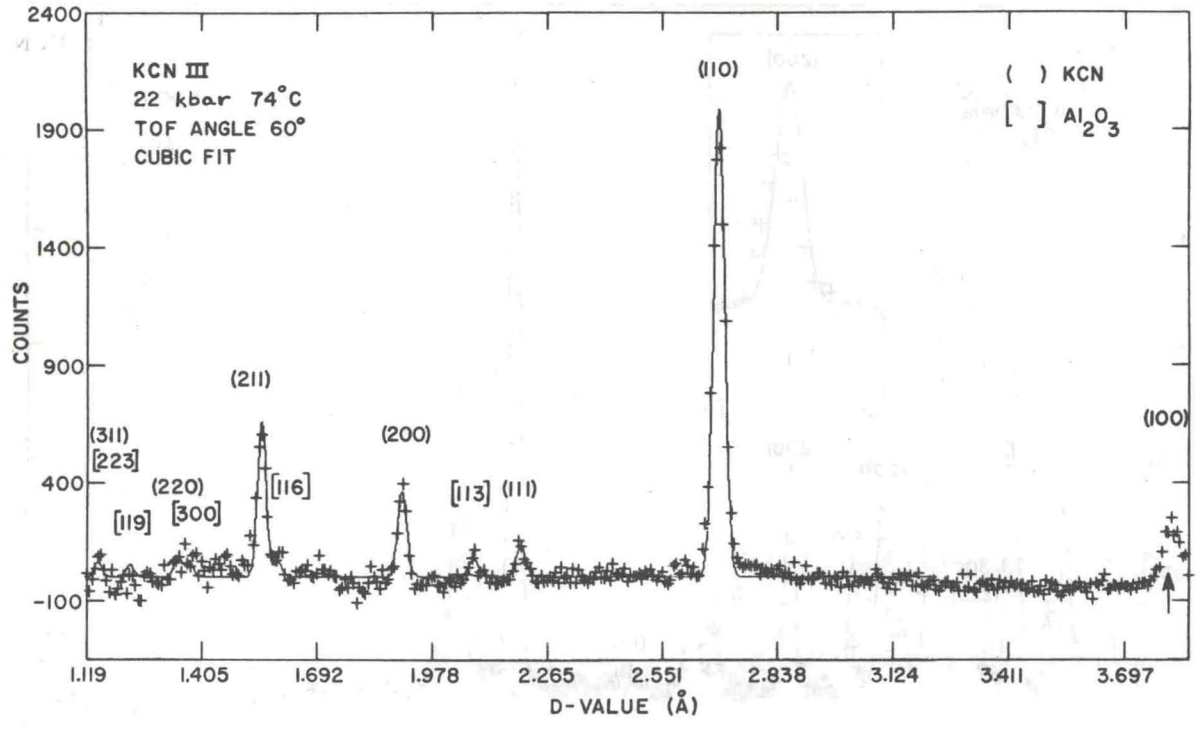

FIG. 2. Time-of-flight (TOF) neutron-diffraction pattern for cubic KCN III with the Maxwellian background mathematically removed. The solid line shows the result of simultaneously fitting all of the peaks using the variable intensity fit as described in Sec. III of the text. The fit is not extended to the (100) peak at the extreme right end of the pattern because of a frame overlap problem which caused the background to rise slightly here. The calculated position of the (100) peak is shown by a vertical arrow. The peaks due to the alumina (Al_2O_3) pressure cell are given with their hexagonal indices.

eters which are the only adjustable parameters affecting the peak positions. $\alpha_{\vec{h}}$ and $f_{\vec{h}}$, are the peak amplitudes of the KCN peaks and the Al_2O_3 peaks, respectively, and v is an overall intensity factor for Al_2O_3. The KCN peak amplitudes $\alpha_{\vec{h}}$ are treated as variable parameters while the relative amplitudes $f_{\vec{h}}$, for Al_2O_3 are held fixed at values determined from a pure Al_2O_3 diffraction pattern. Pb peaks, if present, are treated in the same manner as Al_2O_3 peaks. This allows an accurate subtraction of Al_2O_3 and Pb peaks from the pattern, particularly as these in all cases were very small at the 60° scattering angle. In some regions of the diffraction pattern the intensities obtained from this type of analysis are slightly in error because the assumed shape for the Maxwellian with the three variable parameters is not sufficient to exactly fit the background over the entire spectrum. For the least-squares technique described here, the ratio of χ^2 to the number of degrees of freedom which we shall designate the "goodness of fit" should lie between 0.8 and 1.2 for a perfect statistical fit. In what follows we shall refer to the fit summarized in Eq. (1) as the variable intensity fit.

Since the TOF diffraction method employs a continuous range of neutron wavelengths (λ), the measured intensities are modified by the thermal neutron spectrum and by a λ^4 multiplication.[16] Relative structure factors were determined from the measured intensities $[I_{\vec{h}}^{\mathrm{TOF}} = \alpha_{\vec{h}} S_t (\pi/4 \ln 2)^{1/2}]$ according to the relation

$$m_{\vec{h}} |F_{\vec{h}}|^2 \propto I_{\vec{h}}^{\mathrm{TOF}} / \lambda^4 I_0(\lambda) , \qquad (2)$$

where $m_{\vec{h}}$ is the multiplicity for the peak with label $\vec{h}$ in the diffraction pattern, $F_{\vec{h}}$ is the structure amplitude including Debye-Waller factors, and $I_0(\lambda)$ characterizes the neutron flux from the reactor. In our case $I_0(\lambda)$ was determined from a measurement of the direct beam transmitted through the pressure cell containing the sample using a detector matched to those used for the 30° and 60° scattering angles, and so $I_0(\lambda)$ should implicitly contain absorption and multiple scattering corrections for both the sample and pressure cell as well as detector efficiency corrections. In fits to the diffraction pattern for well-known cubic materials it was found that the measured $I_0(\lambda)$ predicted structure factors for the diffraction peaks associated with the longer neutron wavelengths which were too low. In order to fit the measured intensities

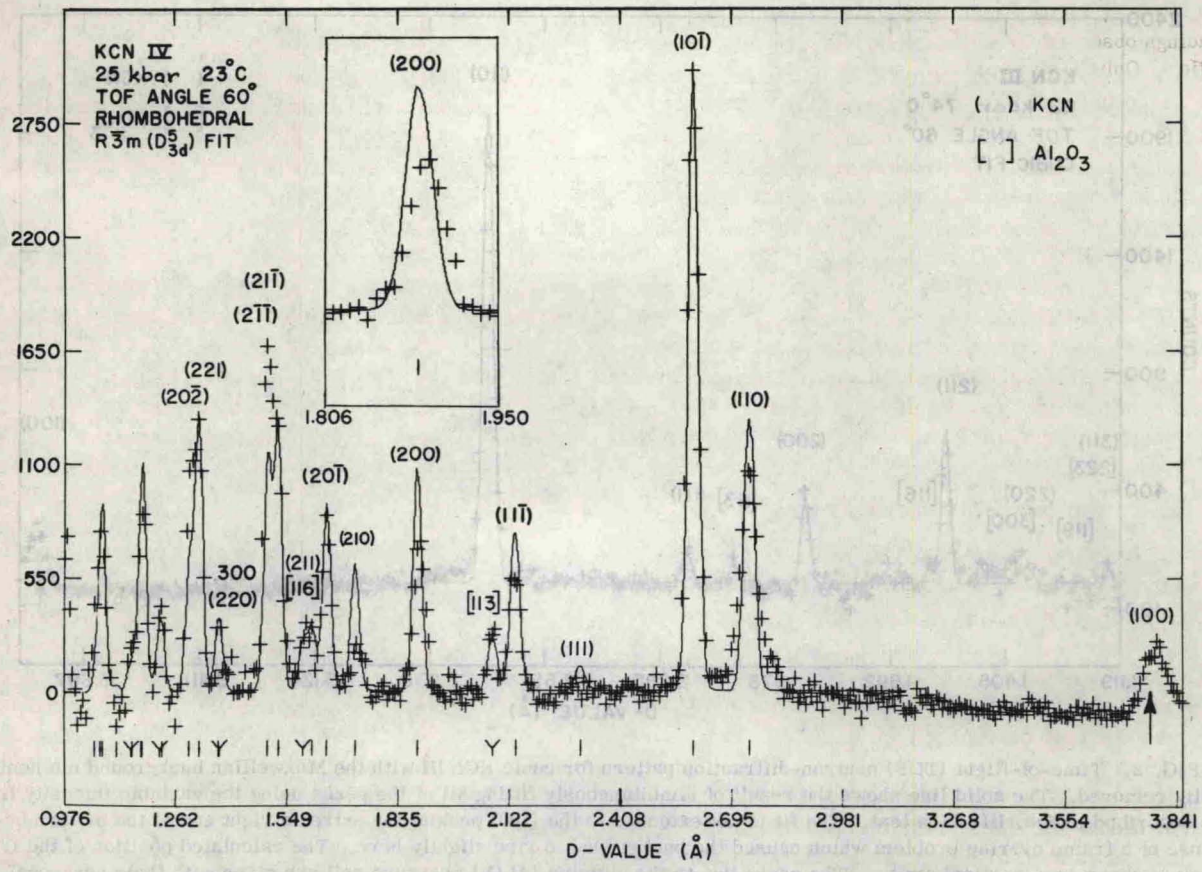

FIG. 3. TOF neutron-diffraction pattern for KCN IV. The solid line shows the result of simultaneously fitting all of the peaks assuming the space group $R\bar{3}m(D_{3d}^5)$ with the cyanide ion lying along the primary axis of the rhombohedral unit cell. (See Sec. III of the text.) The displacement of the (100) and the (200) peaks from their exact rhombohedral positions is emphasized by the inset above the (200) peak and the vertical arrow showing the calculated position of the (100) peak. The vertical lines just below the diffraction pattern give the rhombohedral line positions while the positions of the observable Al_2O_3 lines are marked by the symbol *Y*.

TABLE I. Plane spacing and intensity of KCN III at 74 °C and 22 kbar.

cubic *hkl*	d_{obs}[a] (Å)	d_{calc} (Å)	$m\|F_{hkl}\|^2_{obs}$	$Pm3m(O_h^1)$	$m\|F_{hkl}\|^2_{calc}$ Free rotation model
100	3.807±0.002	3.8080	16.4±2.9	18.6	18.6
110	2.6912±0.0011	2.6926	82.1±5.6	79.8	79.0
111	2.1982±0.0017	2.1985	5.8±0.5	5.9	3.8
200	1.9049±0.0007	1.9040	14.5±1.7	14.5	16.1
210		1.7030	<2.4	0.4	0.1
211	1.5538±0.0016	1.5546	29.5±2.6	30.9	27.0
220		1.3463	<4.8	7.6	6.0
300, 221	1.2694±0.0028	1.2693	5.2±3.3	5.5	6.4
310		1.2042	<2.0	1.4	7.4
311	1.1498±0.0016	1.1482	9.6±2.4	9.7	8.8
Lattice parameter = 3.8080±0.0003 Å				Refinement fitting parameters	
Unit cell volume = 55.22±0.01 Å^3			B_K(Å^2)	2.6±0.6	2.23
			B_{CN}(Å^2)	3.9±0.8	6.21
			C-N Bond length (Å)	1.23±0.02	1.2
			R value for fit (%)	4.1	11.5

[a]No entry in column 2 signifies that it was not intense enough to determine *d*-spacing.

TABLE II. Calculated and measured positions for the spacings observed in KCN IV assuming a rhombohedral lattice. Only those peaks which could be resolved are listed. Lattice parameters $a_{hex} = 5.1906 \pm 0.0007$ Å, $c_{hex} = 6.9129 \pm 0.0023$ Å, $a_{rh} = 3.780$, and $\alpha_{rh} = 86°42'$. Volume of rhombohedral unit cell = 53.77 ± 0.03 Å^3.

hexagonal indexing	Rhombohedral indexing	d_{calc} (Å)	d_{obs} (Å)
101	100	3.7685	3.783 ± 0.002
012	110	2.7400	2.7405 ± 0.0011
110	$10\bar{1}$	2.5953	2.5954 ± 0.0004
003	111	2.3043	...
021	$11\bar{1}$	2.1375	2.1363 ± 0.0069
202	200	1.8842	1.8909 ± 0.0006
113	210	1.7231	1.7291 ± 0.0020
211	$20\bar{1}$	1.6500	1.6502 ± 0.0007
122	$21\bar{1}$	1.5248	1.5250 ± 0.0007
300	$2\bar{1}\bar{1}$	1.4984	1.4981 ± 0.0005
015	221	1.3215	1.3210 ± 0.0007
220	$20\bar{2}$	1.2976	1.2980 ± 0.0009

for well-known cubic materials, the measured $I_0(\lambda)$ was adjusted for the longer neutron wavelengths by dividing it by $[1 + (\lambda - 1.8)]^{1/2}$ for $\lambda > 1.8$ Å and by unity for $\lambda \leq 1.8$ before using it in Eq. (2) to calculate relative structure factors. We are not sure why this empirical correction is necessary, but different detector efficiencies could account for it.

In further analyzing the data for KCN IV, we modified the least-squares-fitting technique summarized in Eq. (1) in order to test particular space groups. In this case the term $\alpha_{\vec{h}}$ for the amplitude of the KCN peak with label $\vec{h}$ is replaced by the expression

$$\alpha_{\vec{h}} \rightarrow [\mu \lambda_i^4 I_0(\lambda_i)/S_i]\, m_{\vec{h}} |F_{\vec{h}}|^2 , \qquad (3)$$

where μ is an over-all intensity scaling factor for KCN and the relative intensities for the peaks are no longer arbitrary but fixed by the chosen space group. This analysis was particularly useful in refining the KCN IV structure since the KCN IV diffraction pattern contained overlapping peaks.

Since the intensity measurements are important to our interpretation of the diffraction patterns for the high-pressure phases we measured the intensities for the KCN I pattern at room temperature (see Table III) and compared them with the powder diffraction results in the literature.[7,17,18] These measurements were taken with the sample inside the pressure cell before application of pressure. We have scaled the results so that the TOF value for the intensity ($|F|^2$) of the (200) diffraction peak agrees with the literature value.[7,17,18] The good agreement with intensities obtained in previous powder neutron-diffraction studies confirms the accuracy of our spectrum determination and the validity of the empirical correction discussed earlier.

For the KCN III pattern (Fig. 2) the diffraction peaks were well resolved and the peaks could be analyzed separately using Eq. (1) to determine the best value for the intensity of each peak. For the (110) diffraction peak there appear to be some small intensity "wings" above the background which may be due to thermal diffuse scattering, but no explicit allowance was made for this in the intensity analysis. The relative structure factors $|F_{\vec{h}}|^2$ computed according to Eq. (2) were analyzed with a refinement program[19] to determine the position of the CN^- ion in the unit cell and the Debye-Waller factors for the K^+ and CN^- ions. Scattering lengths of $b_K = 0.37$, $b_C = 0.665$, and $b_N = 0.94$ in units of 10^{-12} cm per atom were assumed for the respective nuclei.[20]

Two different models were tried in the effort to determine the nature of the disordering among the linear CN^- molecules within the cubes formed by the K^+ ions in KCN III. Following Richter and Pistorius[6] we first tried the space group $Pm3m(O_h^1)$ in which the K^+ ions were placed at the origin and the C and the N atoms were averaged over the eight equivalent (g) positions at x_1, x_1, x_1 along the [111] directions in the cubic unit cell. The eight CN scattering centers were each assigned a scattering length of $\frac{1}{8}(b_C + b_N)$. The midpoint of the CN bond was fixed at $(\frac{1}{2}, \frac{1}{2}, \frac{1}{2})$. In the refinement calculation[19] the thermal factors B_K, B_{CN} are given by the quantity $\exp[-B(h^2 + k^2 + l^2)/4a^2]$ in the expression for the structure amplitude where a is the lattice parameter for KCN III. The results of the refinement fitting are given in Table I. The position of the CN group resulting from the refinement was $x_1 = 0.4071 \pm 0.0017$ yielding a C-N bond length of 1.23 ± 0.02 Å along one of the [111] directions. The thermal factors $B_K = 2.6 \pm 0.6$ Å^2 and $B_{CN} = 3.9 \pm 0.8$ Å^2 are quite large, reflecting the large amount of molecular libration present in this disordered system. Using the relation

$$B_{K,CN} = 8\pi^2 \langle \mu_x^2 \rangle_{K,CN} , \qquad (4)$$

the linear motional amplitude $\langle \mu_x^2 \rangle^{1/2}$ is 0.18 and 0.23 Å for the K^+ and CN^- ions, respectively. The R value for the first ten peaks, of which only seven are clearly visible above the background was 4.1%. The large thermal factors reduced the amplitude of the peaks associated with smaller lattice spacings below the statistical fluctuation in the background.

Next we tried a "free-rotation" model[17] in which

the K^+ ions were again fixed at the origin and the CN group was treated as a single entity which moved freely on the surface of a sphere whose center was at $(\frac{1}{2}, \frac{1}{2}, \frac{1}{2})$ and whose radius was one-half the CN bond length. The best fit resulted for bond lengths in the range 1.20~1.24 Å. The results for the fit with a bond length of 1.2 Å are tabulated in Table I. The R value for this fit was $R = 11.5\%$ which is to be compared with $R = 4.1\%$ for the fit to $Pm3m(O_h^1)$. The "free-rotation" model appears to be a much less satisfactory model for KCN III.

IV. ANALYSIS OF THE KCN IV PATTERN

The rhombohedral analysis of the KCN IV data exposed two serious problems. First, several of the diffraction peaks were broadened in excess of the instrumental broadening with shapes that were not truly Gaussian, so that the fitting program summarized in Eq. (1) could not be used to compare intensities. Second, although the observed diffraction peak positions for KCN IV given in Table II were very nearly consistent with a rhombohedral lattice with unit-cell constants $a_{rh} = 3.780$ Å, $\alpha_{rh} = 86.7°$, the (100), (200), and (210) diffraction peaks were displaced from their rhombohedral positions by more than the experimental uncertainty.

On the basis of high-pressure x-ray measurements, Pistorius[5] concluded that the most likely space group for KCN IV was $R\bar{3}m(D_{3d}^5)$. Here the K^+ ion is at (0, 0, 0) and the cyanide ion lies along the [111] rhombohedral axis but without distinction between the heads and tails of the CN^-'s. Using the modification of our fitting program summarized in Eq. (3) we tested this model. The CN^- group was treated as a single entity with a scattering length $b_{CN} = \frac{1}{2}(b_C + b_N)$. This "CN atom" was placed at $\pm(0, 0, z)$ in the hexagonal cell in which the c axis coincides with the [111] axis of the rhombohedral cell. The K^+ ion was placed at the origin as before. The expression for the structure amplitude in Eq. (3) becomes

$$F_{\vec{h}} = (b_K e^{-B_K/4d_h^2} + b_{CN} e^{-B_{CN}/4d_h^2} \times 2\cos 2\pi lz) \times \{1 + 2\cos[\tfrac{2}{3}\pi/(-h+k+l)]\}. \quad (5)$$

The fitting yielded a value for z of 0.4037 ± 0.0012, implying a CN bond length of 1.33 ± 0.02 Å. The results for the temperature factors for the K^+ ions and the CN^- group were, respectively, $B_K = 1.7 \pm 0.4$ Å^2, $B_{CN} = 5.0 \pm 0.3$ Å^2. The solid line in Fig. 3 represents the best fit of the KCN IV diffraction pattern to $R3m(D_{3d}^5)$. The poor intensity agreement apparent from the figure is reflected in the rather large goodness-of-fit value, 8.93 (See Sec. III). The displacement of the (100) and (200) diffraction peaks from their exact rhombohedral positions and the apparent line broadening for several of the diffraction peaks [(100), (110), and (200)] which was apparent in the fitting procedure summarized by Eq. (1) (no constraints on intensities) is also evident in Fig. 3. The errors given are statistical and do not reflect these problems in the fitting.

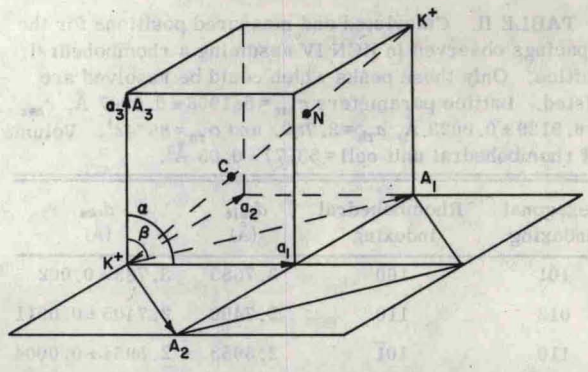

FIG. 4. Relation of the crystallographic unit cells for KCN III and KCN IV. $\vec{a}_1$, $\vec{a}_2$, $\vec{a}_3$ are the edges of the cubic cell for KCN III. $\vec{A}_1$, $\vec{A}_2$, and $\vec{A}_3$ are the edges of the C-centered monoclinic cell derived from the rhombohedral cell which results from the application of a small rhombohedral distortion to the cubic cell. The monoclinic cell for KCN IV may be pictured as the result of a rhombohedral distortion followed by a monoclinic distortion as described in the text. The C and N atoms, shown as lying along a [111] axis in the above figure, lie in ordered positions in the A_1A_3 plane in the monoclinic cell of KCN IV.

The diffraction peak broadening discussed above could arise either from a domain size effect[21] based on a short-range ordering of the CN^- molecule or from a distortion of the rhombohedral lattice to lower symmetry. The displacement of the (100) and (200) peaks from their positions in the rhombohedral lattice constitutes a strong argument for the latter explanation.

Since these displacements are small, the distortion from the rhombohedral structure must be small. The rhombohedral cell constants indicate only a slight distortion from the cubic structure of KCN III, and it is therefore convenient to start from the model sketched in Fig. 4 where $\vec{a}_1$, $\vec{a}_2$, and $\vec{a}_3$, ($a = 3.808$ Å) form the edges of the cubic cell. Here the C and N atoms are placed along a threefold [111] axis in the cubic cell consistent with the fact that the space group $R\bar{3}m(D_{3d}^5)$ with the cyanide ions lying along the rhombohedral axis enables a reasonably good description of the observed intensities (Fig. 3). The $R\bar{3}m(D_{3d}^5)$ space group can be generated by increasing the length of the cube diagonal so that the angle α is smaller than 90° ($\alpha = 86.7°$). This is accompanied by a decrease of a to 3.780 Å to agree with the rhombohedral lattice parameter. The vectors $\vec{a}_1$, $\vec{a}_2$, and $\vec{a}_3$ now become the basis vectors of the rhombohedral cell. We can describe this structure in terms of a monoclinic cell with

TABLE III. Comparison of time-of-flight intensity measurements on KCN I with previous powder diffraction results.

hkl	$\|F\|^2$(TOF)	$\|F\|^2$[a]
111	1.8±0.2	2.16
200	5.7±0.5	5.72
220	3.7±0.3	3.40
311	0.31±0.06	0.25
222	1.9±0.2	2.11

[a]Reference 7.

the basis $\vec{A}_1 = \vec{a}_1 + \vec{a}_2$, $\vec{A}_2 = \vec{a}_1 - \vec{a}_2$, and $\vec{A}_3 = \vec{a}_3$. We now have a C-centered monoclinic structure with two molecules per cell and CN^- lying in the (010) plane.

The nature of the monoclinic distortion from the rhombohedral structure can be inferred from the fact that no "peak broadening" was observed for diffraction from the rhombohedral $(10\bar{1}) \leftrightarrow$ hexagonal (110) planes which are parallel to the [111] diagonal of the rhombohedral unit cell while broadening was observed for diffraction from the rhombohedral (110), (100), and (200) planes which intersect the [111] axis. In the monoclinic cell which coincides with the undistorted rhombohedral cell (Fig. 4) this implies a distortion of $\vec{A}_1$ and $\vec{A}_3$, in the plane perpendicular to A_2, but no change in $\vec{A}_2$, which is perpendicular to the [111] rhombohedral axis. Such a distortion of $\vec{A}_1$ and $\vec{A}_3$ will change the symmetry from rhombohedral to C-centered monoclinic, but will not alter the plane spacing of planes which are parallel to the [111] rhombohedral axis.

There are three centered monoclinic space groups $C2(C_2^3)$, $C2/m(C_{2h}^3)$, and $Cm(C_s^3)$ which are subgroups of $R3m(D_{3d}^5)$. $C2(C_2^3)$ and $C2/m(C_{2h}^3)$ give completely wrong diffraction intensities for all allowable positions of C and N and so the final choice is the space group $Cm(C_s^3)$ with the C and N nuclei in the A_1A_3 plane of Fig. 4 which includes the [111] rhombohedral axis. In what follows we describe the monoclinic cell with the parameters, a, b, c, and $\cos\beta$ where $A_1 = a$, $A_2 = b$, $A_3 = c$, and $\cos\beta = (\vec{A}_1 \cdot \vec{A}_3)/ac$.

A fit to the KCNIV diffraction pattern based upon the space group $Cm(C_s^3)$ was made using the modification of the least-squares-fitting technique described in Eq. (3) with the carbon nuclei at $(x_C, 0, z_C)$ and the nitrogen nuclei at $(x_N, 0, z_N)$. Symmetry requires that the C and N atoms lie in the plane perpendicular to the unique monoclinic b axis. This is a more general requirement than that indicated by their location along the primary rhombohedral axis of the undistorted cell shown in Fig. 4. The structure factor $|F_{\vec{h}}|^2$ in Eq. (4) becomes

$$|F_{\vec{h}}|^2 = A_{\vec{h}}^2 + B_{\vec{h}}^2 ,$$

with

$$A_{\vec{h}} = b_K e^{-B_K/4d_{\vec{h}}^2} + [b_C \cos 2\pi(hx_C + lz_C) + b_N \cos 2\pi(hx_N + lz_N)]\, e^{-B_{CN}/4d_{\vec{h}}^2},$$

and

$$B_{\vec{h}} = [b_C \sin 2\pi(hx_C + lz_C) + b_N \sin 2\pi(hx_N + lz_N)]\, e^{-B_{CN}/4d_{\vec{h}}^2} . \quad (7)$$

In the monoclinic cell $d_{\vec{h}}$ in Eq. (1) becomes[22]

$$d_{\vec{h}} = (1 - \cos^2\beta)^{1/2} \times \left(\frac{h^2}{a^2} + \frac{k^2(1-\cos^2\beta)}{b^2} + \frac{b^2}{c^2} - \frac{2hl\cos\beta}{ac} \right)^{1/2} . \quad (8)$$

All other parameters in Eq. (7) have been previously described. In the computer fit summarized in Eqs. (1), (4), and (7), the parameters a, b, c, and $\cos\beta$, the lattice parameters for Al_2O_3, u, v, x_C, z_C, x_N, z_N, B_K, B_{CN}, α, γ, and δ were varied to yield the best least-square fit to the data. This gives ten KCN crystal parameters to be determined from 53 peaks in the monoclinic structure. Most of these peaks are overlapping pairs or triplets but this analysis technique can readily handle overlapping peaks. The results for the diffraction pattern taken at 25 kbar and 23 °C are shown in Fig. 5 and Table IV. The monoclinic structure seems to account very well for the diffraction line positions. The value obtained for the monoclinic cell angle, $\cos\beta = 0.0771 \pm 0.0003$ (Table IV), rules out the possibility that the unit cell for KCNIV is orthohombic. However, some intensity discrepancies appear in the fit using the space group $Cm(C_s^3)$. It is evident from Fig. 5 that the observed intensity for the (002) peak of the monoclinic pair (002), (220) is significantly lower than allowed in the best fit (solid line). The inset at the lower right-hand side of Fig. 5 showing a restricted region of the fit to the data for the 30° scattering angle shows the same discrepancy for the (001) peak of the monoclinic pair (001), (110). The experimentally observed intensity for the monoclinic pairs of diffraction lines labeled (401), (312) and (200), (111) in Fig. 5 is larger than allowed in the fit to $Cm(C_s^3)$. The discrepancy for the (401), (312) and (200), (111) monoclinic pairs is far more serious in the fit to the diffraction pattern of KCNIV collected at 34 kbar and 23 °C where it is also apparent that the observed intensity of the (400), (222) monoclinic pair is larger than allowed in the fit to C_s^3. These discrepancies might be due to the presence of preferred orientation which, in view of the latter observations, must become more pronounced with pressure. It is known that application or reduction of pressure in a solid pressure medium can give rise to preferred orientation. Indeed, we found

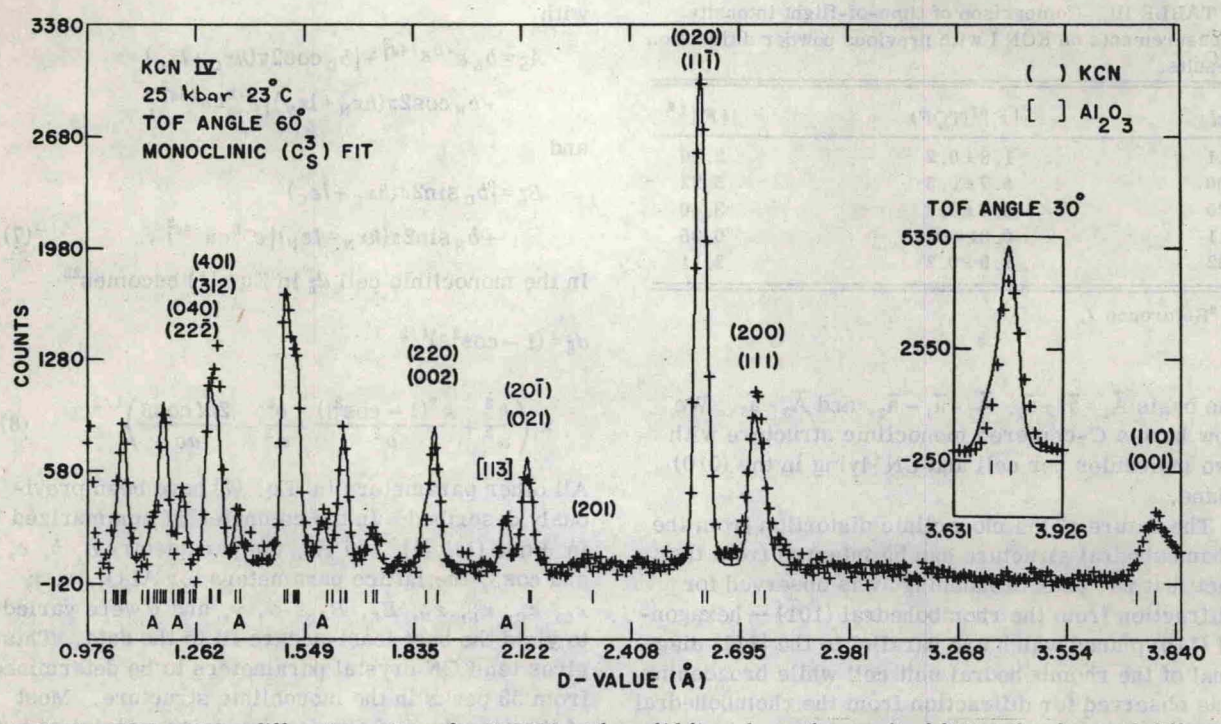

FIG. 5. TOF neutron-diffraction pattern for KCN IV. The solid line shows the result of fitting the observed diffraction pattern assuming that KCN IV is described by the centered monoclinic space group $Cm(C_c^3)$ (see Sec. IV). The inset above and to the left of the (001), (110) monoclinic pair shows the result of doing the above fit to the data for the 30° scattering angle. The vertical lines just below the diffraction pattern give the monoclinic line positions while the position of the observable Al_2O_3 lines due to the pressure cell are marked by the symbol A.

that, after release of pressure, the intensities observed for the (111) and (222) peaks in KCN I were reduced by a factor of 2 with respect to their values prior to the application of pressure (Table III) while the intensities for the other peaks remained unchanged.

The temperature factors for the K^+ and CN^- ions, B_K and B_{CN}, are smaller in KCN IV than in KCN III, indicating that the ordering of the CN^- molecules is more complete in this phase. The value for B_{CN} in the fit to the diffraction pattern collected at 25 kbar, 23 °C ($B_{CN}=2.8$ Å^2, Table IV) gives a linear motional amplitude for the CN ion $\langle\mu_{x'}^2\rangle_{CN}^{1/2}\sim 0.19$ Å [Eq. (4)], which is to be compared with the values $B_{CN}=4.0$ Å^2, $\langle\mu_{x'}^2\rangle_{CN}^{1/2}\sim 0.24$ Å for KCN III. The value for B_K in phase IV is essentially zero in contrast to the large $B_K=2.7$ Å found in phase III. (The fact that the thermal factor for the potassium ion B_K has been set equal to zero in each of the above fits means that, in the course of the fitting, the statistical error for this parameter exceeded its value.) An explanation for this result is sug-

TABLE IV. Results of C_s^3 analysis of KCN IV phase.

P,T	25 kbar, 23 °C	34 kbar, 23 °C	22 kbar, 66 °C
Goodness of fit	3.7	5.7	2.0
a	5.5307 ± 0.0013	5.5050 ± 0.0018	5.5166 ± 0.0024
b	5.2093 ± 0.0008	5.1885 ± 0.0011	5.2662 ± 0.0022
c	3.7431 ± 0.0009	3.7286 ± 0.0012	3.7579 ± 0.0020
$\cos\beta$	0.0771 ± 0.0003	0.0825 ± 0.0004	0.0596 ± 0.0007
½ Unit cell Volume (Å^3)	53.76 ± 0.03	53.07 ± 0.05	54.49 ± 0.07
Carbon x,z	0.426 ± 0.008, 0.365 ± 0.008	0.434 ± 0.010, 0.366 ± 0.014	0.429 ± 0.008, 0.350 ± 0.011
Nitrogen x,z	0.583 ± 0.006, 0.544 ± 0.006	0.587 ± 0.007, 0.563 ± 0.010	0.570 ± 0.006, 0.514 ± 0.011
B_K(Å^2)	0.0	0.0	0.0
B_{CN}(Å^2)	2.84 ± 0.23	1.52 ± 0.29	4.56 ± 0.24
C-N bond length (Å)	1.14 ± 0.06	1.16 ± 0.09	1.02 ± 0.08

gested by the argument that KCN III is similar to KCN I in which the large motional amplitude for the K^+ ions appears to be associated with the local dilatations accompanying the rotational motions of the CN^- ion.[4] In KCN IV the ordering of the CN^- molecules is more complete, and it is likely that these rotational motions are largely absent. Consequently, the local dilatations of the K^+ ions should be absent also.

Results for the computer fit to a third diffraction pattern for KNC IV (22 kbar, 66 °C) are also summarized in Table IV. The value obtained for the monoclinic cell angle, $\cos\beta = 0.0596 \pm 0.0007$, when compared with the corresponding value from the measurement at 25 kbar 23 °C, $\cos\beta = 0.0771 \pm 0.0003$, shows that the distortion from the cubic KCN III structure decreases as the IV-III phase boundary is approached. The small value for the C–N bond length, 1.02 ± 0.08 Å has a large uncertainty associated with it and is suspect due to the presence of weak KCN III peaks in the KCN IV diffraction pattern.

An attempt was also made to fit the KCN IV data (25 kbar 23 °C) using the rhombohedral space group $R3m(C_{3v}^5)$. This introduces an additional positional parameter in comparison with the fit to $R\bar{3}m(D_{3d}^5)$ since the C and N positions are now allowed to vary independently. However, the fit was different from that described for the space group $R\bar{3}m$ insofar as the fitting program was modified to include the effect of preferential line broadening due to a domain size effect following an analysis procedure for domain line broadening for single-crystal x-ray diffraction carried out by Evenson and Barnett.[21] Although the resultant fit reproduced the observed line shapes very well it could not account for the displacement of observed peak positions discussed above. This fit also could not account for the observed intensity of the diffraction line with rhombohedral indices (221). This is the discrepancy already pointed out in the monoclinic analysis, since the monoclinic pair (401), (312) corresponds to the rhombohedral (221) line in the undistorted cell. The goodness-of-fit ratio for this analysis (5.3) was significantly worse than the corresponding ratio for the monoclinic analysis (3.7).

V. DISCUSSION AND CONCLUSION

The KCN III phase seems to be understood reasonably well. The crystal structure is cubic with the space group $Pm3m(O_h^1)$. The diffraction peak intensities are well represented assuming a disordered crystal with the CN^- ion randomly distributed over the eight diagonal configurations. The temperature factors are unusually large indicating a high probability of the CN^- ion jumping between equilibrium positions. The large motional amplitude for the K^+ ions may be caused by local dilatations accompanying the rotational motions of the CN^- ion. This dynamical picture is very similar to that proposed for KCN I.[4]

The KCN IV phase is more difficult to interpret definitively. There is some displacement of the (100) and (200) peaks from their exact rhombohedral positions (~0.014 and 0.007 Å, respectively) which, although small, is well outside the accuracy of the experiment. This indicates some distortion of the rhombohedral structure. A centered monoclinic lattice with the space group $Cm(C_s^3)$ gives a good fit to the diffraction pattern.

Two features of the monoclinic analysis of the KCN IV phase stand out. First, the C and N atoms are ordered in the $Cm(C_s^3)$ space group, in which ferroelectricity is allowed. Possible evidence for this is the fact that the (200), (111) monoclinic pair shows line broadening in excess of the instrumental line width (Fig. 5), which may be due to the presence of domains in the monoclinic structure, with the implication of ferroelectric behavior. Second, the temperature factors for the K^+ and CN^- ions B_K and B_{CN}, are smaller in KCN IV than KNC III. The large temperature factors in KCN III are probably due in large part to the molecular libration which is present in this disordered system, so it is not surprising that the value for B_{CN} decreases upon passing to KCN IV where the CN molecules are much more ordered. It seems likely that the rotational motions of the rod-shaped CN molecules are largely absent in KCN IV. This would imply the absence of the local dilatations of the K^+ lattice present in a disordered system as KCN I.[4] This picture is consistent with our result that $B_K \approx 0$ in KCN IV.

Some intensity discrepancies remain. For the two orders of the (001), (110) monoclinic pair which were observed, the observed intensity for the (001) line is lower than allowed by the fit using the space group $Cm(C_s^3)$. The calculated intensities for the monoclinic pairs (401), (312) and (200), (111) which are not in particularly good agreement with the diffraction pattern collected at 25 kbar and 23 °C (Fig. 5) give a very poor fit to the diffraction pattern collected at 34 kbar, which also shows a similar discrepancy for the second-order reflection of the (200), (111) pair. These discrepancies may indicate the presence of preferred orientation in KCN IV or may be due to an inadequacy in the assumed model.

Results for measurements in phase IV at two different temperatures (Table IV) indicate that the C–N bond length may contract as the temperature is increased in phase IV. However, the value for the bond length obtained from the measurement at higher temperature (1.02 ± 0.08 Å) has a large uncertainty associated with it and is suspect due to the presence of weak KCN III peaks in the KCN IV

diffraction pattern. Further increase of the temperature results in the transformation into the cubic phase III in which the C–N bond length has lengthened to 1.23 ± 0.02 Å, a value which is slightly higher than the original value for the bond length 1.14 ± 0.06 Å in phase IV at room temperature. This result could be independently checked by infrared spectroscopy. It is also apparent from Table IV that the C and N nuclei lie nearly along the body diagonal of a slightly distorted cube of K^+ ions in the C_s^3 structure. This is exactly the case if $x_N = z_N$ and $x_C = z_C$ and even though the ratio of x/z in these analyses was completely free the best fit to that data gives a value close to unity.

ACKNOWLEDGMENTS

We wish to thank W. E. Evenson and J. D. Barnett for providing us with a copy of their domain-broadening theory prior to publication and we wish to thank Sherman Susman for the KCN sample material. One of us (D. L. D) wishes to express thanks to the Office of Educational Affairs at Argonne for the fellowship which allowed him to work on this project at Argonne. One of us (G. R.) would like to express his appreciation to Argonne National Laboratory for the opportunity to stay at Argonne while this project was carried out.

---

*Based on work performed under the auspices of U. S. Atomic Energy Commission.

†Present address: Dept. of Physics and Astronomy, Brigham Young University, Provo, Utah 84602.

‡Present address: Centre d'Etudes Nucleaires de Grenoble, Avenue Des Martyrs-38-Grenoble, France.

[1]P. W. Bridgman, Proc. Am. Acad. Arts Sci. 72, 45 (1937).

[2]C. W. F. T. Pistorius, J. B. Clark, and E. Rapoport, J. Chem. Phys. 48, 5123 (1968).

[3]H. Suga, T. Matsuo, and S. Seki, Bull. Chem. Soc. Jpn. 38, 1115 (1965).

[4]D. L. Price, J. M. Rowe, J. J. Rush, E. Prince, D. G. Hinks, and S. Susman, J. Chem. Phys. 56, 3697 (1972).

[5]C. W. F. T. Pistorius, J. Phys. Chem. Solids 32, 2761 (1971).

[6]P. W. Richter and C. W. F. T. Pistorius, Acta. Crystallogr. B 28, 3105 (1972).

[7]M. Atoji, J. Chem. Phys. 54, 3514 (1971).

[8]This is argued from an assumed $R \ln 8$ configurational entropy in phase III and the change in entropy from slope and volume change along the III–IV boundary.

[9]G. Roult, R. Beyerlein, D. Decker, and T. G. Worlton, Bull. Am. Phys. Soc. 18, 35 (1973).

[10]R. M. Brugger, R. B. Bennion, and T. G. Worlton, Phys. Lett. A 24, 714 (1967).

[11]D. G. Hinks, D. L. Price, J. M. Rowe, and S. Susman, J. Cryst. Growth 15, 227 (1972).

[12]R. M. Brugger, R. B. Bennion, T. G. Worlton, and W. R. Myers, Trans. Am. Crystallogr. Assoc. 5, 141 (1969).

[13]D. L. Decker, J. Appl. Phys. 42, 3239 (1971).

[14]D. L. Decker and T. G. Worlton, J. Appl. Phys. 43, 4799 (1972).

[15]The lattice parameters of Ge and Si were taken to be 5.65754 and 5.4307 Å, respectively.

[16]B. Buras, Nukleonika 8, 259 (1963).

[17]N. Elliott and J. Hastings, Acta. Crystallogr. 14, 1018 (1961).

[18]A. Sequeira, Acta. Crystallogr. 18, 291 (1965).

[19]W. R. Busing, K. O. Martin, and H. A. Levy, Report No. ORNL-TM-305, Oak Ridge National Laboratory, Oak Ridge, Tennessee, 1964 (unpublished).

[20]G. E. Bacon, Acta. Crystallogr. A 25, 391 (1969).

[21]W. E. Evenson and J. D. Barnett (unpublished).

[22]*International Tables for X-ray Crystallography* (Kynoch, Birmingham, England, 1965), Vol. I.